Hindawi
Advances in Civil Engineering
Volume 2020, Article ID 5749685, 9 pages
https://doi.org/10.1155/2020/5749685

Research Article

Bending Properties of Short-Cut Basalt Fiber Shotcrete in Deep Soft Rock Roadway

Shaoyang Yan,[1,2] Huazhe Jiao ,[1,2] Xiaolin Yang,[1,2] Jinxing Wang,[1,2] and Fengbin Chen[1,2]

[1]*School of Civil Engineering, Henan Polytechnic University, Jiaozuo 454000, China*
[2]*Henan Key Laboratory Underground Engineering and Disaster Prevention, School of Civil Engineering, Henan Polytechnic University, Jiaozuo 454000, China*

Correspondence should be addressed to Huazhe Jiao; jiaohuazhe@126.com

Received 15 October 2019; Revised 8 June 2020; Accepted 16 June 2020; Published 14 July 2020

Academic Editor: Valeria Vignali

To study the effect of short-cut basalt fiber (BF) on the bending and toughening properties of shotcrete, bending toughness tests of short-cut BF shotcrete slabs with different volume fractions were carried out. A transparent soil model and Scanning Electron Microscopy (SEM) were used to observe the distribution of BF with different volume fractions and analyze the toughness enhancement mechanism of basalt fiber shotcrete. The supporting effect of basalt fiber shotcrete with different volume fractions was verified by an underground engineering test. The test results show the following: (1) when the fiber content is within 3~4.5 kg/m^3, the distribution of BF in transparent soil is uniform, and it does not easily agglomerate, which is beneficial to improving the bending toughness of shotcrete. (2) The shotcrete slab with 4.5 kg/m^3 fiber content had the best reinforcing effect. Compared with the control group, the peak load and absorption capacity increased by 56.67% and 636.96%, respectively, and the maximum crack width decreased by 32.10%. (3) The SEM analysis indicated that the basalt fibers distributed randomly and evenly in the concrete, which can form a three-dimensional spatial skeleton with a stable structure. Excessive fiber incorporation can increase fiber agglomeration during stirring and spraying. (4) The support results of an underground engineering test show that, in 35 days, short-cut basalt fiber shotcrete with 4.5 kg/m^3 fiber content is better at restraining the surrounding rock than shotcrete with other fiber contents. BF has the properties of crack resistance, bridging, and toughening for shotcrete and can significantly improve the ability of shotcrete to restrain surrounding rock deformation. As a new type of fiber, BF has great significance in deep soft rock underground engineering.

1. Introduction

Surrounding rock stability control is one of the important research areas in the field of deep soft rock underground engineering, especially for practical problems such as difficult control of the surrounding rock stability and large deformation in the deep 800~2000 m high-stress condition [1, 2]. Traditional shotcrete has some shortcomings, such as small elongation, poor crack resistance, and high brittleness, which reduce the support effect and seriously endanger the stability of the surrounding rock structure and personal safety [3, 4]. Basalt fiber (BF) is a new fiber material with a high inorganic environmentally friendly green performance. Compared with other fibers (glass fiber and steel fiber), basalt fiber has better corrosion resistance, a higher elastic modulus, better chemical stability, impact resistance, and fire resistance [5, 6]. Basalt fiber was originally used in military and aerospace research programs [7, 8] and is now widely used as a structural reinforcement material in buildings [9–11], bridges [12, 13], highways [14, 15], tunnels [16, 17], and other fields. Basalt fibers have the functions of crack resistance, bridging, and toughening in concrete, which can significantly improve the fatigue resistance, post-cracking toughness, and durability of the concrete [18–20].

In recent years, domestic and foreign scholars have carried out a large number of experimental studies on fiber reinforced concrete. Sim et al. [21] found that the toughness of basalt fiber reinforced concrete is 3~5 times higher than that of ordinary concrete. Zhang et al. [22] suggested that basalt fibers could improve the toughness and crack resistance

of concrete through experiments. Pickel et al. [23] tested the mechanical properties of basalt fiber reinforced concrete with different content. The basalt fibers were found to generally increase the tensile and flexural strength (modulus of rupture), and it was found on inspection that the fibers had ruptured upon macrocracking. Ayub et al. [24] suggested that the addition of basalt fibers significantly increased the tensile splitting strength and the flexural strength of HPFRC and slightly improved the compressive strength. Attia K et al. [25] found that basalt fiber can improve the bending resistance of the concrete sheet strips. Abed and Alhafiz [26] researched the effects of adding different types of fibers to the concrete mixtures on the flexural behaviour of concrete beams, which were reinforced longitudinally with BFRP bars. Their results showed that basalt fibers can improve the bending resistance of these beams. Wang et al. [27] found that the bonding between the fibers and concrete matrix is the main factor that improves the effect of the strengthening and toughening of fiber reinforced concrete. Iyer [28] conducted mechanical property tests on concrete with different lengths and quantities of basalt fiber and found that clumping of fibers at a high fiber content will cause mixing and casting problems. Li et al. [29] studied the effect of hybrid fibers on the flexural toughness of concrete square slabs and beams and used European and American codes to evaluate the flexural toughness characteristics. Li et al. [30] studied the early strength of steel fiber shotcrete slabs with different content according to the European EFNARC standard and found that steel fiber can significantly improve the impact resistance of early concrete. However, the research on the bending characteristics and strengthening and toughening of BF shotcrete is not perfect, so it is necessary to study the application of BF shotcrete in deep soft rock underground engineering.

At present, the research on the bending characteristics and strengthening and toughening effect of BF shotcrete is limited to the laboratory only, and the research results cannot be used in underground engineering. Therefore, this paper studies the influence of short-cut BF shotcrete slabs with different volume fractions on the bending characteristics and toughness by using a test of underground shotcrete slabs. The distribution of fiber in the shotcrete and the strengthening and toughening mechanism are investigated and analyzed by means of a transparent soil model and SEM technology. Finally, a field test is used to systematically monitor the convergence deformation of different volumes of BF sprayed concrete, to verify the support effect.

2. Experimental Materials and Methods

2.1. Experimental Materials and Mix Proportion. The experimental materials are as follows: PO 42.5R Portland cement produced by Qianye Cement Plant; the coarse aggregate is calcareous macadam with a mud content of 0.2 and maximum particle size of 10 mm; fine aggregate is manufactured sand with fineness modulus of 3 and particle size of 0~3 mm; short-cut BF with 18 mm fiber, with parameters as shown in Table 1. The accelerator is Xingde Brand accelerator, Wuan City, Hebei Province, and the water is tap water from Jiaozuo City. The specimen mix is shown in Table 2.

2.2. Experimental Methods

2.2.1. Fiber-Transparent Soil Model Experiment. To prepare the fiber-transparent soil model, different sizes of quartz sand were mixed in the mixer for 30 seconds, adding different amounts of short-cut basalt fiber, stirring for 40 seconds, pouring the stirred mixture into a plexiglass box ($100 \times 100 \times 100$ mm), and then adding the refractive index 1.4585 calcium bromide solution prepared by using an abbe refractometer. The distribution of different fiber content in transparent soil was observed. The fiber-transparent soil model was binarized by Image J software, and the fiber distribution was counted.

2.2.2. Bending Toughness Experiment of Shotcrete Slab. According to the European EFNARC standard for making $600 \times 600 \times 100$ mm shotcrete slab [31], specimens with fiber volume fractions of 0 kg/m^3, 3 kg/m^3, 4.5 kg/m^3, and 6 kg/m^3 were made in the bottom drainage roadway of Zhaogu No.2 coal mine, respectively, while square slabs with fiber volume fractions of 0 kg/m^3 were used as the control group. Three parallel specimens were made for each group. The specimens were demoulded 24 hours later and kept underground for 28 days before being transported to the laboratory for testing.

The flexural toughness test of the shotcrete slabs is divided into three steps. Step one: place the square slab on the rigid frame, and place a $100 \times 100 \times 100$ mm loading rigid block at the centre of the specimen. Step two: apply load with a TAW-3000G electrohydraulic servo high rigid pressure testing machine, with a loading speed of 1.5 mm/min. Step three: the CY050-2A deform meter (range 50 mm) and crack width gauge were used to monitor and record the load and deflection of the centre slab, the deformation of the centre bottom slab, and the crack width and extension crack width of the loading specimen. The flow of the square slab test is shown in Figure 1.

2.2.3. SEM Experiment. For choosing failure specimens to conduct SEM, in order to ensure focused scanning, the test pieces were sliced and selected to be placed in a sample bag for keeping. The enclosed sample was taken out during the test and fixed on the sample stage with a conductive paste. The sample stage to which the sample is fixed is placed in an ion sputtering equipment for gold coating. Then, the SEM instrument switch is turned on, the appropriate beam spot value is selected, and a SEM test is performed.

3. Experimental Results and Analysis

3.1. Distribution of BF in Transparent Soil Model with Different Contents. The fiber-transparent soil model was divided into 9 cells, binary analysis was conducted by Image J software, and the visible fiber distribution in different cells was counted. The distribution morphology of fiber with each content in the transparent soil model is shown in Figure 2, and

Table 1: Physical and mechanical properties of basalt fiber.

Material	Diameter (μm)	Length (mm)	Density (g/cm^3)	Tensile strength (MPa)	Modulus of elasticity (GPa)	Elongation at fracture (%)
Basalt fibers	13	18	2.65	4100~4800	80~100	2.7~3.4

Table2: Shotcrete mix of experimental specimens (kg/m^3).

Cement	Coarse aggregate	Fine aggregate	Water	Accelerator	Early strength agent
440	880	880	260	17.6	2.2

(a) (b) (c) (d)

Figure 1: Production of shotcrete specimen. (a) On-site fabrication of square boards. (b) Site maintenance. (c) Demoulding and maintenance. (d) Slab pressing.

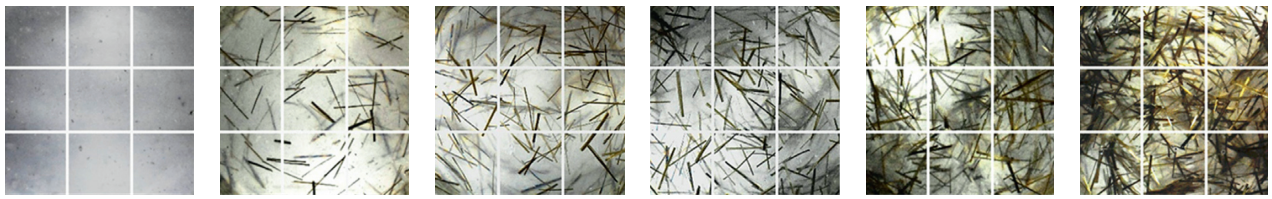

(a) (b) (c) (d) (e) (f)

Figure 2: Fiber-transparent soil model with different content. (a) 0 kg/m^3. (b) 1.5 kg/m^3. (c) 3 kg/m^3. (d) 4.5 kg/m^3. (e) 6 kg/m^3. (f) 7.5 kg/m^3.

the binarization image of the fiber distribution in the transparent soil is shown in Figure 3.

In order to quantitatively evaluate the dispersion of fiber in the transparent soil, the dispersion coefficient of fiber is proposed, and its expression is shown in the following formula:

$$\beta = \exp - \left[\sum \left(\frac{(X_i / X_i)}{T} \right]^{(1/2)} \right. . \quad (1)$$

In the formula, T is the number of cells in the field of view, X_i ($i = 1 \sim 9$) is the number of fibrous roots in different cells, X_a is the average number of fibrous roots in all cells in the entire image, and β is the dispersion coefficient of the fiber.

Define the dispersion coefficient of the weighted average value of the content of BF contribution value $\alpha_j (\alpha_0 = 1)$ and the contribution growth coefficient $\gamma_j (j = 1 \sim 5)$, where j corresponds to (1.5, 3, 4.5, 6, and 7.5 kg/m^3), five kinds of contents, respectively. Its expression is shown in the following formulas:

$$\alpha_j = V_f \cdot \beta_j, \quad (2)$$

$$\gamma_j = \frac{\alpha_j - \alpha_{j-1}}{\alpha_{j-1}}. \quad (3)$$

V_f is the BF content and β_j is the BF dispersion coefficient. The dispersion of different content of BF in the transparent soil is shown in Table 3.

According to Table 3, the BF content has a great influence on the fiber distribution. When the content is 1.5 kg/m^3, the fiber dispersion coefficient is 0.7 and the fiber contribution rate is 0.05. In the transparent soil model, the fiber distribution is random, with large gaps, and a uniform network structure cannot be formed. When the content is 3 kg/m^3, the fiber dispersion coefficient is 0.76 and the fiber contribution rate is 1.171. The gaps between fibers are small, and multiple fibers are connected to form a stable spatial network structure. A few bubbles appear in the transparent soil model. When the fiber content is 4.5 kg/m^3, the fiber dispersion coefficient is 0.52, and the fiber contribution rate is 0.026, which indicates fiber agglomeration. When the fiber content is 6.0 kg/m^3, the fiber

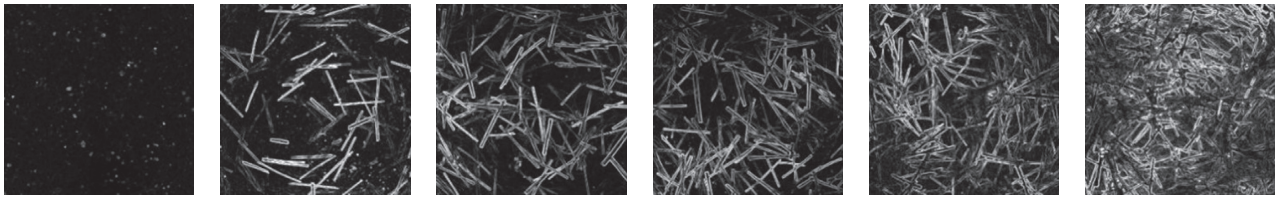

(a) (b) (c) (d) (e) (f)

Figure 3: Binarization model of fiber-transparent soil with different content. (a) 0 kg/m^3.(b) 1.5 kg/m^3.(c) 3 kg/m^3. (d) 4.5 kg/m^3.(e) 6 kg/m^3. (f) 7.5 kg/m^3.

Table 3: The dispersion of different content of BF in transparent soil.

Specimen	Fiber content (kg/m^3)	Visible fiber number	Distribution situation	Dispersion coefficient	Fiber contribution growth coefficient
P0	0	0	0	—	—
P1	1.5	67	Large fiber spacing	0.7	0.05
P2	3	126	Moderate fiber spacing	0.76	1.171
P3	4.5	158	Uniform distribution of fiber spacing	0.52	0.026
P4	6	196	Uneven distribution of fibers	0.46	0.179
P5	7.5	237	Poor fiber distribution	0.37	0.005

dispersion coefficient is 0.46 and the fiber contribution rate is 0.179. The fiber distribution is uneven and bubbles in the model increase greatly.

It can be seen that the proper amount of fiber can exert a gain effect, and the excess fiber is entangled and overlapped. When the fiber dispersion amount is 3~4.5 kg/m^3, the BF distribution uniformly forms a dense network structure, which is less prone to clumping and has a small overlap ratio. This is beneficial to improving the bending toughness of the sprayed concrete.

3.2. Effect of BF on Bidirectional Reinforcement Mechanism and Toughness of Shotcrete Square Slab

3.2.1. Effect of BF on Bidirectional Reinforcement Mechanism of Shotcrete Square Slab. The load-deflection curves of simply supported BF shotcrete square slabs under concentrated loads can be divided into the elastic stage, stress redistribution stage, and unloading stage. The load-deflection curve of a square slab with 4.5 kg/m^3 content is shown in Figure 4.

Elastic stage (OA segment) [32]: with the increase of load, the two-way bending moment of the slab increases continuously. When the bending moment is less than the ultimate bending moment (M_1) of the square slab, there is no cracking in the square slab and it is approximately elastic. When the unidirectional bending moment reaches the maximum bending moment (the load reaches point A), a unidirectional microcrack appears at the bottom of the square slab.

Stress redistribution stage (ABCDE segment) [33]: this stage can be divided into an internal microstructure effect (AB) stage and a BF effect (BE) stage. AB segment: under the condition of external force, the defects such as microcrack and pore expansion within the square slab leads to a decrease of the bearing capacity. BE segment: with the increase of

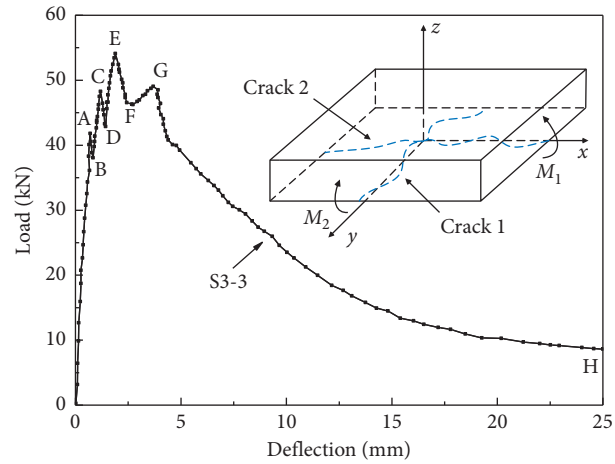

Figure 4: The load-deflection curve of a square slab with 4.5 kg/m^3 content.

load, the bonding effect between the fiber and matrix delays the development of cracks and increases the bearing capacity.

Unloading stage (EFGH segment) [30]: after reaching the peak load of 54.11 kN, the crack develops into a main crack penetrating the matrix of the shotcrete square slab. The bridging fibers under the effect of tension are pulled out of the matrix of the shotcrete square slab, and the bearing capacity of the slab decreases to 46.27 kN (EF segment). Before the fiber reaches its ultimate tensile strength, its own strength enhances the bearing capacity of the concrete matrix, and the bearing capacity increases to 49.06 kN (FG segment). The fracture of the bridging fibers leads to a sharp decline in the bearing capacity of the square slab until it is destroyed (GH segment).

3.2.2. Comparative Analysis of Bending Properties of Square Slab with BF Content. The results of the mechanical properties of the basalt fiber shotcrete square slabs are shown

Table 4: Test results of mechanical properties of BF reinforced concrete square slabs.

Content of BF (kg/m^3)	Specimen	Initial cracking deflection (mm)	Initial crack load	Average value	Peak deflection (mm)	Peak load (kN)	Average value	Residual load (kN)	Average value
0	S1-1	0.74	33.86	34.67	0.74	33.86	34.67	0.0	0.00
	S1-2	0.67	34.56		0.82	34.56		0.0	
	S1-3	0.81	35.60		1.10	35.60		0.0	
3	S2-1	1.30	40.66	39.55	1.75	43.35	43.51	2.98	3.37
	S2-2	1.28	39.42		1.88	44.62		3.52	
	S2-3	1.13	38.56		1.68	42.57		3.62	
4.5	S3-1	0.94	46.82	46.80	1.80	53.51	53.22	8.62	8.48
	S3-2	0.87	45.36		1.74	52.04		8.50	
	S3-3	1.18	48.23		1.89	54.11		8.33	
6	S4-1	0.74	38.62	40.01	1.52	45.51	45.19	5.45	5.11
	S4-2	0.82	40.87		1.49	46.02		5.02	
	S4-3	0.81	40.53		1.60	44.05		4.86	

in Table 4 and Figure 5 which indicate that the peak loads of shotcrete square slabs with fiber content of 0 kg/m^3, 3 kg/m^3, 4.5 kg/m^3, and 6 kg/m^3 are 34.67 kN, 43.51 kN, 53.22 kN, and 45.19 kN, respectively. The variance of the peak loads is 0.5110, 0.8091, 0.7562, and 0.6970, respectively. It can be seen from the variance of the different fiber content that the fluctuation of the test data is small, indicating that the dispersion of the test data is good. Compared with the control group, the peak loads with fiber contents of 3 kg/m^3, 4.5 kg/m^3, and 6 kg/m^3 increased by 11.11%, 56.67%, and 32.21%, respectively. The control group shotcrete square slab has high brittleness and low toughness. With the addition of BF to the shotcrete concrete, the ultimate load and toughness of the concrete can be improved appropriately.

In order to study the effect of different contents of basalt fibers on the toughness of the square slabs, the energy absorption value in the EFNARC standard is used to characterize the fracture toughness of the slabs. The calculation method is as follows:

$$W = \int_0^{\delta} F(x)\mathrm{d}x. \tag{4}$$

In the formula, W is the square slab energy absorption value (unit: J); δ is the central deflection of the square slab; and $F(x)$ is the load corresponding to the central deflection of the square slab X.

According to the load-displacement curves of shotcrete square slabs with different contents of basalt fiber in Figure 5, the energy absorption values corresponding to different deflections are obtained by the integral method, as shown in Table 5. The energy absorption curve is shown in Figure 6.

Figure 6 shows that the energy absorption capacity of square slabs with fibers of 3 kg/m^3, 4.5 kg/m^3, and 6 kg/m^3 is 322.08 J, 565.10 J, and 373.23 J, respectively. Compared with the control group (76.68 J), the energy absorption capacity increased by 320.03%, 636.96%, and 386.74%, respectively. Therefore, BF can significantly improve the toughness and energy absorption capacity of BF shotcrete.

Through the analysis of the load-deflection curve and energy absorption curve, it can be seen that the square slab with the 4.5 kg/m^3 volume fraction of fiber shows the highest toughness and energy absorption capacity.

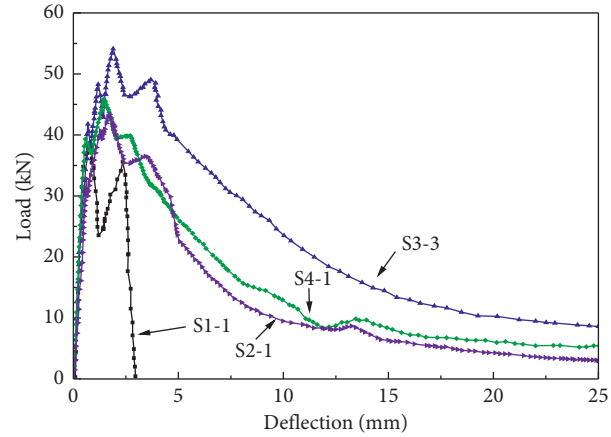

Figure 5: Load-deflection curve of BF shotcrete square slab.

3.2.3. Analysis of Failure Form of Shotcrete Square Slab. The crack development law and failure pattern of basalt fiber shotcrete square slab are shown in Table 6 and Figure 7.

The conclusions drawn from Table 6 and Figure 7 are as follows.

The BF shotcrete square slabs have four cracks for each amount, and the fiber contents are 0 kg/m^3, 3 kg/m^3, 4.5 kg/m^3, and 6 kg/m^3, where the mean values of the corresponding crack width are 0.28 mm, 0.25 mm, 0.19 mm, and 0.23 mm, respectively, compared with the control group. The crack width reduced by 10.7%, 32.1%, and 17.9%, respectively. With the increase of fiber content, the crack width of the square slab first increases and then decreases. The bridging effect of the fiber creates a bond between the fiber and the concrete matrix, which causes the stress redistribution and limits the generation and expansion of the crack. Therefore, increase of the fiber content is beneficial to limiting the development of the crack in the square slab and appropriately raises its bearing capacity and ductility. However, excessive fiber content increases the porosity

Table 5: Effect of BF on energy absorption of shotcrete square slabs.

Specimen	Energy absorption value (J)									
	$\delta = 2.5$	$\delta = 5.0$	$\delta = 7.5$	$\delta = 10.0$	$\delta = 12.5$	$\delta = 15.0$	$\delta = 17.5$	$\delta = 20.0$	$\delta = 22.5$	$\delta = 25.0$
S2-1	87.09	158.57	209.31	243.37	264.82	277.01	285.52	294.10	304.27	322.08
S3-3	108.72	211.85	296.73	363.26	418.23	462.53	497.25	522.55	545.26	565.10
S4-1	93.10	170.45	227.34	267.63	294.01	313.08	327.14	338.92	353.30	373.23

δ is the centre deflection of shotcrete square slab (mm).

inside the concrete matrix, resulting in a decrease in the toughness of the matrix.

The failure mode of the control group was brittle failure with a flat fracture surface. When the flexural specimens of plain sprayed concrete were destroyed, the cracks developed rapidly. With the addition of BF, the toughness of the basalt fiber shotcrete square slab was improved, the crack interface of the square slab was not intersected at the centre point, and the fracture interface appeared as an irregular fracture shape. When the fiber content is 4.5 kg/m^3, the average crack width is the smallest, and the irregularity of cracks is poor. Combined with the analysis of the load and energy absorption of the slabs, the peak load value and energy absorption value are maximum of the slabs. The bridging connection provided by the basalt fiber across the crack can effectively improve the toughness and maximum elongation of the shotcrete square slab, avoiding sudden brittle fracture after the peak load of the slab, and making the slab gradually transition from brittle failure to ductile failure.

3.3. SEM Analysis. Electron microscopic scanning is an effective method to study the internal distribution and microstructure of cement-based hydration products [34, 35], allowing the observation of the distribution of fibers and the bonding mode between fibers and matrix and analyzing the effect of hydration products such as ettringite and C-S-H on the microstructure of the fiber matrix. The bonding mode of the fiber matrix is shown in Figure 8.

Figure 8 shows that the basalt fibers are covered with dense cement hydration matrix, so there is a good chemical cementation between the fibers and the matrix (Figure 8(a)). The basalt fibers are distributed randomly and evenly in the concrete, which can form a three-dimensional spatial skeleton with a stable structure (Figure 8(b)). Excessive fiber incorporation can increase fiber agglomeration during stirring and spraying, which may reduce the bonding property between BF and shotcrete matrix (Figure 8(c)). Once a new crack appears in the specimen under external loads, the fiber spanning the crack consumes energy to restrain the crack development through the debonding and slipping of the fiber, thus delaying the driving force of crack propagation in the concrete (Figure 8(d)).

When the existing crack driving force is restrained and energy accumulates in the concrete, the anisotropic distribution of the BF will seek new cracks in the weak points of the matrix to release energy again. The toughness and strength of concrete is enhanced by the fiber skeleton distributed inside the concrete. The effect of single BFs dispersed in basalt fiber shotcrete is similar to reinforcing bars. The secondary micro-reinforcement

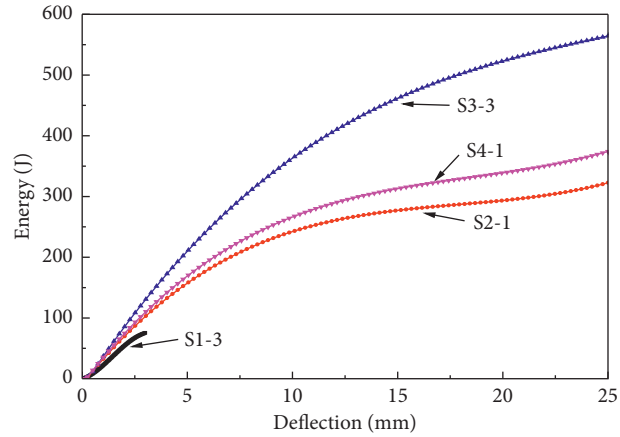

Figure 6: Energy absorption curve.

effect of BF combined with shotcrete matrix can effectively improve the mechanical properties of basalt fiber shotcrete.

4. Field Application of BF Shotcrete

4.1. Engineering Background. The short-cut basalt fiber shotcrete is applied to the bottom extraction roadway of Zhaogu No.2 coal mine (the roadway elevation is −848~−850 m). The test section of roadway is located in the fractured shatter zone. Because of the action of the fault zone, the marl fracture zone in the test section of the roadway is well developed. The surrounding rock of the roadway has a weak layer and a strong water-rich layer. The lithology soft easy to produce large deformation (the maximum deformation of the support is 300 mm). Concrete cracking and detachment, deformation of steel support, and other phenomena occur very often, resulting in the failure of supports, a great threat to mine safety. Therefore, the short-cut basalt fiber shotcrete was used for the field test, and 200 m of the bottom extraction roadway was selected for the underground support test. Every 40 m, a different fiber content was selected for the bolt-shotcrete support. After the shotcrete was completed, two sets of monitoring points were used to monitor the convergence deformation of the roadway. The layout of the convergence survey points in the bottom drainage roadway is shown in Figure 9.

4.2. Analysis of Convergence Deformation of Roadway. After the basalt fiber shotcrete has set and hardened, convergence deformation monitoring is carried out for 35 days on the bottom drainage roadway. The monitoring results are shown in Figure 10. The addition of BF increases the deformation resistance of the supporting structure. The

Table 6: Crack development law of BF shotcrete square slabs.

Content of BF (kg/m^3)	Specimen	Maximum width of initial crack (mm)	Average value	Crack reduction rate (%)	Limit crack width (mm)	Average value	Crack reduction rate (%)	Maximum crack width (mm)	Average value	Crack reduction rate (%)
0	S1-1	0.18	0.19	—	0.28	0.28	—	0.28	0.28	—
	S1-2	0.19			0.26			0.26		
	S1-3	0.20			0.30			0.30		
3	S2-1	0.18	0.18	5.3	0.25	0.25	10.7	0.28	0.27	3.6
	S2-2	0.19			0.23			0.25		
	S2-3	0.18			0.26			0.28		
4.5	S3-1	0.13	0.14	26.3	0.18	0.19	32.1	0.22	0.22	21.4
	S3-2	0.14			0.20			0.23		
	S3-3	0.14			0.18			0.20		
6	S4-1	0.16	0.15	21.1	0.21	0.23	17.9	0.24	0.26	7.1
	S4-2	0.14			0.23			0.26		
	S4-3	0.15			0.24			0.28		

(a) (b) (c) (d)

Figure 7: Failure modes of shotcrete slabs with different BF contents. (a) 0 kg/m^3.(b) 3 kg/m^3. (c) 4.5 kg/m^3.(d) 6 kg/m^3.

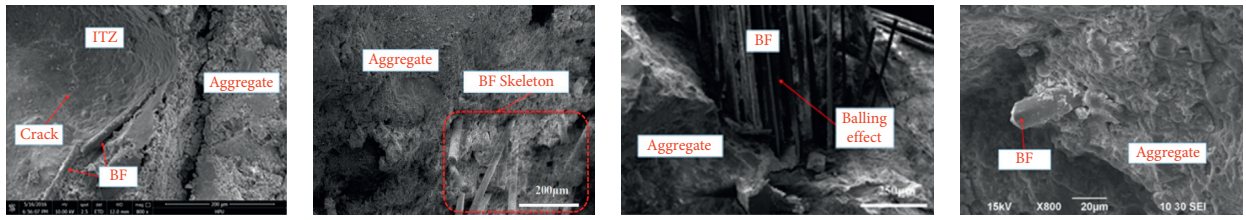

(a) (b) (c) (d)

Figure 8: Bonding mode of fiber substrate. (a) Matrix around fibers. (b) Fiber random dispersion. (c) Fiber dense distribution. (d) Fiber breakage under stress.

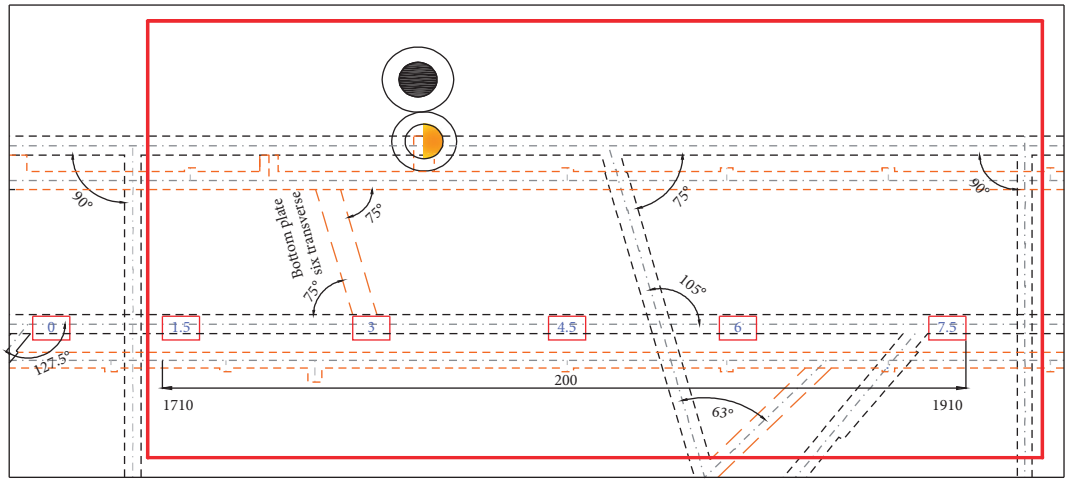

Figure 9: The layout of convergence survey points in the bottom drainage roadway.

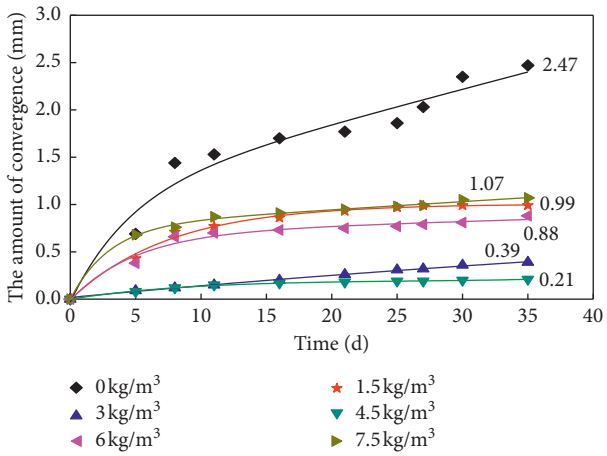

Figure 10: Convergence deformation curve of bottom drainage roadway.

maximum deformation (7 days) of the plain sprayed concrete retaining structure is 1.44 mm. When the BF content is 3 kg/m^3 and 4.5 kg/m^3, the deformation of the roadway is only 0.12 mm in the first 7 days. The total convergence displacement of the plain sprayed concrete at 35 days is 2.47 mm. When the BF content is 4.5 kg/m^3, the convergence displacement of the bottom drainage roadway is 0.21 mm. In the stirring and spraying process, the uniformly distributed BF will form a stable bearing structure inside the basalt fiber shotcrete matrix, thereby improving the resistance of the roadway to deformation.

5. Conclusions

In this paper, the effect of BF on the flexural toughness of shotcrete square slab is studied. The fiber-reinforced mechanism is analyzed by means of a synthetic fiber-transparent soil model and SEM technology, combined with a field test, and the following conclusions are drawn:

(1) Through the fiber-transparent soil model, it is found that when the fiber content is within 3~4.5 kg/m^3, the distribution of BF is uniform and it forms a dense network structure, in which agglomeration appears and has a small ratio of pores, which is beneficial to improving the bending toughness of the shotcrete concrete.

(2) According to the comparison test of the bending toughness of the square slab, it is found that when the fiber content is 4.5 kg/m^3 it had the best reinforcing effect. Compared with the control group, the peak load and absorption capacity increased by 56.67% and 636.96%, respectively, and the maximum crack width decreased by 32.10%.

(3) The SEM analysis indicated that the three-dimensional random distribution of BF forms a stable load-bearing skeleton in the shotcrete, improves the stress distribution in the shotcrete matrix, reduces the crack driving force, and restrains the generation and development of microcracks. Excessive fiber incorporation can increase fiber agglomeration during stirring and spraying, which may make BF and shotcrete matrix not fully bonded, and affect the toughness of basalt fiber shotcrete.

(4) BF shotcrete has achieved a good support effect in a deep soft rock underground engineering test: the basalt fiber shotcrete support effect is improved compared with plain shotcrete, and the ability of restraining the deformation of surrounding rock is enhanced. The convergence displacement of the plain shotcrete support section is 2.47 mm in 35 days, while the convergence displacement of the roadway in the basalt fiber shotcrete support section with a fiber dissolution of 4.5 kg/m^3 is only 0.21 mm.

Data Availability

The data used to support the findings of this study are available from the corresponding author upon request.

Conflicts of Interest

The authors declare that there are no conflicts of interest regarding the publication of this paper.

Acknowledgments

This study was supported by the National Natural Science Foundation of China (51874123 and 51834001), the Scientific and Technological Research Projects of Henan Province China (182102310012), and Support Plan for Scientific and Technological Innovation Talents in Colleges and Universities of Henan Province China (19HASTIT047).

References

[1] J. C. Wang, F. Liu, and L. Wang, "Sustainable coal mining and mining sciences," *Journal of China Coal Society*, vol. 41, no. 11, pp. 2651–2660, 2016, in Chinese.

[2] E. S. Bernard, "Age-dependent changes in post-crack performance of fibre reinforced shotcrete linings," *Tunnelling and Underground Space Technology*, vol. 49, pp. 241–248, 2015.

[3] M. Khooshechin and J. Tanzadeh, "Experimental and mechanical performance of shotcrete made with nanomaterials and fiber reinforcement," *Construction and Building Materials*, vol. 165, pp. 199–205, 2018.

[4] J. M. Guo and Y. S. Zhang, "Application research on mine-used high performance polymer modified concrete," *Journal of Mining & Safety Engineering*, vol. 28, no. 4, pp. 660–665, 2011, in Chinese.

[5] C. High, H. M. Seliem, A. EL-Safty, and S. H. Rizkalla, "Use of basalt fibers for concrete structures," *Construction and Building Materials*, vol. 96, pp. 37–46, 2015.

[6] F. Akhlaghi, R. Eslami-Farsani, and S. Sabet, "Synthesis and characteristics of continuous basalt fiber reinforced aluminum matrix composites," *Journal of Composite Materials*, vol. 47, no. 27, pp. 3379–3388, 2012.

[7] V. I. Kostikov, *Soviet Advanced Composites Technology Series: Fibre Science and Technology: Basalt Fibres and Articles Based on Them*, pp. 581–605, Springer, Moscow, Russia, 1995.

[8] S. M. R. Khalili, M. Najafi, and R. Eslami-Farsani, "Effect of thermal cycling on the tensile behavior of polymer composites

reinforced by basalt and carbon fibers," *Mechanics of Composite Materials*, vol. 52, no. 6, pp. 807–816, 2017.

[9] W. W. Hu, H. W. Liu, D. F. Zhao, and Z. B. Yang, "Applications and advantages of basalt assembly in construction industry," *Advanced Materials Research*, vol. 332–334, pp. 1937–1940, 2011.

[10] R. N. Turukmane, S. S. Culhane, and A. M. Daberao, "Basalt-technical fiber for civil applications," *Technische Textilien*, vol. 61, no. 2, pp. 69–71, 2018.

[11] R. H. Wu, "The application of basalt fiber in building materials," *Advanced Materials Research*, vol. 450-451, pp. 499–502, 2012.

[12] T. I. Koval', "Investigation of the reliability of bridge elements reinforced with basalt plastic fibers," *Mechanics of Composite Materials*, vol. 53, no. 4, pp. 479–486, 2017.

[13] X. Wang, Z. Wu, G. Wu, H. Zhu, and F. Zen, "Enhancement of basalt FRP by hybridization for long-span cable-stayed bridge," *Composites Part B: Engineering*, vol. 44, no. 1, pp. 184–192, 2013.

[14] K. Krayushkina, O. Prentkovskis, A. Bieliatynskyi et al., "Perspectives on using basalt fiber filaments in the construction and rehabilitation of highway pavements and airport runways," *The Baltic Journal of Road and Bridge Engineering*, vol. 11, no. 1, pp. 77–83, 2016.

[15] S. L. Ma, B. Peng, and Z. Huang, "Test and analysis of basalt fiber reinforced concrete's mechanical properties and pavement performance," *Advanced Materials Research*, vol. 671-674, pp. 1291–1296, 2013.

[16] M. Wlodarczyk and I. Jedrzejewski, "Concrete slabs strengthened with basalt fibres - experimental tests results," *Procedia Engineering*, vol. 153, pp. 866–873, 2016.

[17] G. Y. Cui, D. Y. Wang, S. Z. Ni et al., "Model tests bearing characteristics of basalt fiber reinforced concrete tunnel linings," *Chinese Journal of Geotechnical Engineering*, vol. 39, no. 2, pp. 311–318, 2017, in Chinese.

[18] S. K. Sateshkumar, P. O. Awoyera, and T. Kandasamy, "Impact resistance of high strength chopped basalt fibre-reinforced concrete," *Revista De La Construccion*, vol. 17, no. 2, pp. 240–248, 2018.

[19] A. Bentur and S. Mindess, *Fiber Reinforced Cementitious Composites*, Taylor & Francis Group, Abingdon, UK, 2007.

[20] D. P. Dias and C. Thaumaturgo, "Fracture toughness of geopolymeric concretes reinforced with basalt fibers," *Cement and Concrete Composites*, vol. 27, no. 1, pp. 49–54, 2005.

[21] J. Sim, C. Park, and D. Y. Moon, "Characteristics of basalt fiber as a strengthening material for concrete structures," *Composites Part B: Engineering*, vol. 36, no. 6-7, pp. 504–512, 2005.

[22] L. F. Zhang, Y. L. Yin, J. W. Liu et al., "Mecha-nical proporties study on basalt fiber reinforced concrete," *Bulletin of the Chinese Ceramic Society*, vol. 33, no. 11, pp. 2834–2837, 2014, in Chinese.

[23] D. J. Pickel, J. S. West, and A. Alaskar, "Use of basalt fibers in fiber-reinforced concrete," *ACI Materials Journal*, vol. 115, no. 6, pp. 867–876, 2018.

[24] T. Ayub, N. Shafiq, and M. F. Nuruddin, "Mechanical properties of high-performance concrete reinforced with basalt fibers," *Procedia Engineering*, vol. 77, pp. 131–139, 2014.

[25] K. Attia, W. Alnahhal, A. Elrefai, and Y. Rihan, "Flexural behavior of basalt fiber-reinforced concrete slab strips reinforced with BFRP and GFRP bars," *Composite Structures*, vol. 211, pp. 1–12, 2019.

[26] F. Abed and A. R. Alhafiz, "Effect of basalt fibers on the flexural behavior of concrete beams reinforced with BFRP bars," *Composite Structures*, vol. 215, pp. 23–34, 2019.

[27] Q. S. Wang and H. Yao, "Application of reinforced concrete in soft rock tunnel at great depth," *Journal of Mining & Safety Engineering*, vol. 25, no. 2, pp. 184–187, 2008, in Chinese.

[28] P. Iyer, S. Y. Kenno, and S. Das, "Mechanical properties of fiber-reinforced concrete made with basalt filament fibers," *Journal of Materials in Civil Engineering*, vol. 27, no. 11, Article ID 04015015, 2015.

[29] H. G. Li, W. Z. Sun, Q. L. Qiu et al., "Study on flexural toughness property of basalt fiber concrete mixed with steel fiber," *Journal of Highway and Transportation Research and Development*, vol. 33, no. 9, pp. 78–83, 2016, in Chinese.

[30] D. Li and Y. N. Ding, "Effect of steel fiber on biaxial flexural property of TRC with basalt fiber mesh in slab test," *Acta Materiae Compositae Sinica*, vol. 20, no. 1, pp. 78–82, 2017, in Chinese.

[31] EFNARC, *European Specification for Sprayed concrete*, Loughborough University, Louthborough, UK, 1996.

[32] X. D. Wang, W. Z. Zhen, and Y. Wang, "Internal force redistribution of umbonded prestressed concrete edge-supported sl-abs," *Journal of Harbin Institute of Technology*, vol. 47, no. 2, pp. 1–8, 2015, in Chinese.

[33] Z. C. Deng, "Flexural toughness and characterization method of hybrid fibers reinforced ultra-high performance concret-e," *Acta Materiae Compositae Sinica*, vol. 33, no. 6, pp. 1274–1280, 2016, in Chinese.

[34] S. Cao, E. Yilmaz, and W. D. Song, "Evaluation of viscosity, strength and microstructural properties of cemented tailings backfill," *Minerals*, vol. 8, no. 8, p. 352, 2018.

[35] S. M. Song, J. H. Liu, and X. Q. Zhang, "Performance of the cement matrix composite material with rubber powder," *Journal of Wuhan University of Technology*, vol. 19, no. 1, pp. 77–80, 2014.